Journal of Materials Chemistry C

Enhancement of pump efficiency for an organic distributed feedback laser based on holographic polymer dispersed liquid crystal as an external light feedback

Journal:	*Journal of Materials Chemistry C*
Manuscript ID:	TC-ART-03-2015-000731.R1
Article Type:	Paper
Date Submitted by the Author:	19-Apr-2015

Complete List of Authors:	Liu, Lijuan; State Key Laboratory of Applied Optics, Changchun Institute of Optics, Fine Mechanics and Physics, Chinese Academy of Sciences, Xuan, Li; aState Key Laboratory of Applied Optics, Changchun Institute of Optics, Fine Mechanics and Physics, Chinese Academy of Sciences, Zhang, Guiyang; State Key Laboratory of Applied Optics, Changchun Institute of Optics, Fine Mechanics and Physics, Chinese Academy of Sciences, Liu, Minghuan; State Key Laboratory of Applied Optics, Changchun Institute of Optics, Fine Mechanics and Physics, Chinese Academy of Sciences Changchun, China, Hu, Lifa; State Key Laboratory of Applied Optics, Changchun Institute of Optics, Fine Mechanics and Physics, Chinese Academy of Sciences, Liu, Yonggang; State Key Laboratory of Applied Optics, Changchun Institute of Optics, Fine Mechanics and Physics, Chinese Academy of Sciences, Ma, Ji; Kent State University, Liquid Crystal Institute

Enhancement of pump efficiency for an organic distributed feedback laser based on holographic polymer dispersed liquid crystal as an external light feedback

Lijuan Liu[a, b], Li Xuan*[a], Guiyang Zhang[a,b], Minghuan Liu[a,b], Lifa Hu[a], Yonggang Liu[a], and Ji Ma*[a, c]

[a]State Key Laboratory of Applied Optics, Changchun Institute of Optics, Fine Mechanics and Physics, Chinese Academy of Sciences, Changchun, 130033, China; [b]University of Chinese Academy of Sciences, Beijing, 100049, China; [c]Liquid Crystal Institute, Kent State University, Ohio, 44240, USA

*E-mail: jma2@kent.edu; xuanli@ciomp.ac.cn

Abstract

We report a low threshold, high energy conversion organic distributed feedback (DFB) laser based on a holographic polymer dispersed liquid crystal (HPDLC) grating as an external light feedback layer, specifically, by adopting acrylate-based monomer with low functionality and a rubbed polyimide (PI) alignment layer. In such configuration, the phase separated LCs were aligned along the preferred direction, which gave increased refractive index difference between the LC and the polymer, so it can provide better light feedback in HPDLC layer. The pump efficiency for the laser, such as lasing output threshold and conversion efficiency, can be enhanced. The light loss, diffraction efficiency and driving voltage were also investigated for the HPDLC structures to identify the effects of rubbing layer and monomer functionality.

1. Introduction

Distributed feedback (DFB) organic semiconductor lasers (OSLs) have been developed extensively based on their materials and resonator structures. Organic semiconducting materials exhibit strong absorption, wide absorption band, small concentration quenching and capability to easy process.[1] Efficient energy conversion could allow optical pumping by light emitting diodes[2] or inorganic laser

diodes,[3] which is promising for compact lasers applications.[4] DFB structures are favorite resonator geometries due to low thresholds and single longitudinal mode emission as a result of long gain path and high wavelength selectivity.[5] So far, DFB OSLs have already been demonstrated with several approaches, such as electron beam lithography,[6] electron beam lithography,[7] hot embossing,[8] reactive ion etching, liquid imprinting[9] or interference ablation.[10] There are two kinds of structures are commonly used. One is the grating structure engraved on the active layer[11] and the other is the active medium deposited on the corrugated substrate.[12] In these cases, the active layer acts as both gain layer and index modulation layer, which makes the coupling mechanism complex and the design of waveguide core layer such as materials or thickness difficult.

A DFB laser with a single active semiconducting layer as the core layer and a holographic polymer dispersed liquid crystal (HPDLC) grating layer as the external feedback layer has different configuration.[13] We can control the parameters of the active layer (as the gain medium and the waveguide core layer) and the HPDLC grating layer (as feedback layer) separately to adjust the properties of the lasing output for the device.[13a] Liquid crystals (LCs) are optically anisotropic. HPDLC gratings are fabricated by exposing a mixture composed of photosensitive monomer and LC to an interference field created by two coherent laser beams by photo-polymerization induced phase separation (PIPS) method. The alternating layers of polymer and phase separated LC are formed corresponding to the interference patterns.[14,15]

In HPDLCs, the averaged orientation of liquid crystal molecules is aligned along grating vector direction, i.e., orthogonal to the holographic planes.[14] For feedback lights propagating along the grating vector, the refractive index difference comes from polymer (index n_p) and phase separated LC (ordinary index n_o). These two values of index is very close and the typical difference[16] can be as low as 10^{-5}. Thus the effective light feedback for lasing output is not high. In this work, we present a DFB OSL with HPDLC as the external feedback layer. Specially, a rubbed polyimide (PI) layer was adopted on the substrate to control the orientation of the phase separated LCs to increase the refractive index difference in the grating vector direction for light feedback. We also found the effect of PI alignment layer was

related with different functionalities of acrylate monomer(s). Through adopting low functional monomer and using rubbed PI alignment layer, the orientation of phase separated LCs can be along the direction of the holographic planes. Therefore the refractive index difference in HPDLC feedback layer can be increased and the lasing performance can be enhanced.

2. Experimental

2.1 Device structure and materials

The device structure is illustrated in Fig. 1. The core layer of the proposed laser device is made from poly (2-methoxy-5-(20-ethyl-hexyloxy) p-phenyl-enevinylene) (MEH-PPV), which serves as laser gain layer. While the bottom glass substrate and the HPDLC grating layer are used as cladding layers to form HPDLC-grating/MEH-PPV/glass substrate configuration as an asymmetric slab waveguide.[13a] Different from previous reports, we applied polyimide (PI) as an alignment layer to control LC alignment on the other glass substrate in some samples, as illustrated in Fig. 1b. The PI was mechanically rubbed unidirectionally by a piece of velvet cloth along the direction of the holographic planes (z axis). The solution of MEH-PPV (Jilin OLED Material Tech) in xylene (6mg/ml) was deposited onto the bottom glass substrate by spin-coating (2000 rpm). The MEH-PPV layer thickness was controlled at 80 ± 2 nm by spin-coating rate and confirmed by Dektak profilometer. The cells gap, i.e., the thickness of the HPDLC, was controlled by Mylar spacer at 6 μm.

To form HPDLC by photo-induced phase separation method,[15] nematic LC TEB30A (n_o=1.522, n_e=1.529, Δn=0.170, Slichem, 27.5 wt.%), N-vinylpyrrolidone (NVP, Sigma-Aldrich, 10 wt.%) as solvent and chain extender, co-initiator Nphenylglycine (NPG, Sigma-Aldrich, 1.5 wt.%), photo-initiator Rose Bengal (RB, Sigma-Aldrich, 0.5 wt.%) and monomer (60 wt.%) were mixed. In order to study the effect of different monomer functionalities[17], difunctional acrylate monomer phthalic diglycol diacrylate (PDDA, Sigma-Aldrich, 30 wt.%) and penta-functional acrylate monomer dipentaerythritol hydroxyl pentaacrylate (DPHPA, Sigma-Aldrich, 30 wt.%) were adopted in mixture A with monomer functionality of 3.5 while PDDA only (60 wt.%) were prepared in mixture B with monomer functionality of 2. The chemical

structures of DPHPA and PDDA are shown in Fig. 2a and b, respectively. Different samples were prepared, as shown in Table 1. Sample **a1** and **a2** were made from mixture A and sample **b1** and **b2** were made from mixture B. To compare the effect of the PI alignment layer, sample **a2** and **b2** had PI layer on the top glass substrate in the device while sample **a1** and **b1** did not have PI layer in the device.

Table 1 Illustration and properties of samples.

Sample #	Mixture	Top glass substrate	η_p (%)	η_s (%)	η_p / η_s
a1	A	bare glass	56.5	1.3	43.5
a2	A	coated with PI and rubbed	57.2	1.4	40.9
b1	B	bare glass	55.5	2.9	19.1
b2	B	coated with PI and rubbed	1.6	57.3	1/35.8

2.2 HPDLC fabrication and characterization

The mixture is injected into the empty cell by capillary action at room temperature (20-22 ^{o}C) after 12 hr stirring at room temperature and put into the holographic optical field to form HPDLC. The schematic optical setup is shown in Fig. 3. The cell was irradiated in the interference field created by two frequency-doubled, 532 nm continuous Nd-YAG laser beams. By changing the intersection angle (θ) of the two coherent beams,[14,15] the grating period (Λ) can be calculated and controlled according to $\Lambda = \frac{\lambda_{532}}{2\sin(\theta/2)}$. The period of the HPDLC grating was chosen at 590 nm for all the samples, which is used to achieve light feedback in HPDLC via the third Bragg order for the gain MEH-PPV. The intensity of each recording beam was 4 mW/cm^2. The exposure time was 5 min and the cured grating area was 8 mm by 8 mm.

To characterize and compare the properties of HPDLC with different structures, light loss and diffraction efficiency were analyzed. Decreased light loss can improve the energy conversion efficiency

of output laser. Light loss at different polarization states can be also used to indicate the orientation of LC in the HPDLC. To calculate the light loss, during the fabrication process, a circularly polarized He-Ne laser (laser-1) was directed onto the sample at normal direction after a polarizer (polarizer-1). Through rotating the polarizer-1, the light loss (L') at *s* or *p* polarization state is derived by $L' = (I_t - I_d)/I_t$. Here I_t is the intensity of He-Ne laser-1 passing through the sample before grating being fabricated and I_d is the intensity of He-Ne laser-1 detected by detector-1 in real time.

The diffraction efficiency of each sample was measured by another He-Ne laser. The laser beam from He-Ne laser-2 was incident onto the sample at the exact Bragg angle and the first order diffracted beam was measured by the detector-2. The Bragg diffraction angle were about 32^o for our samples. The diffraction efficiency is defined as the diffracted light intensity in the first order divided by the incident light intensity. By rotating the polarizer-2, we can get diffraction efficiency at *s* polarization state (η_s) or *p* polarization state (η_p).

2.3 Lasing output performance

The holographical cured samples were then photo-pumped by a Q-switched frequency-doubled Nd:YAG laser (532 nm, 8 ns, 1 Hz). The pump beam was divided into two beams with equal intensity by a beam splitter. One beams was directed into a pulse energy meter and the other beam was shaped into a narrow strip (5 mm by 0.1 mm) by a cylindrical lens to the sample along the direction of grating vector to pump the laser emission. The lasing output was detected and measured by a fiber pigtail detector coupled spectrometer (LabMax-TOP; Coherent Inc). The lasing output, such as full width at half maximum (FWHM) and lasing threshold can be obtained.

3. Results and discussion

3.1 Scattering loss in HPDLC

The scattering loss can be used to determinate the goodness of HPDLC grating as a feedback layer for

lasing output. The lower the scattering loss, the more efficient the pump light, i.e., the higher conversion efficiency of pump input to the lasing output. The scatting loss in different polarization states can also give clues on LC orientation because the scattering is mainly induced by phase separated LC, which the refractive index of phase separated LC mismatches with the refractive index of environment of the polymer. Fig. 4 shows the scattering loss change with the HPDLC curing time for sample **a1-b2**. From Fig. 4a-c, we can see the scattering loss for *p* polarization light was greater than that for *s* polarization light for sample **a1, a2** and **b1** while from Fig. 4d, the scattering loss for *s* polarization light was larger than that for *p* polarization light. The scattering loss difference for different polarization states indicates that the LC orientation in the HPDLC is different. We will discuss this in Section 3.2.

3.2 Diffraction efficiency for HPDLC

Fig. 5 shows the real-time diffraction efficiencies of each sample at different polarization states. We can see that Fig. 5a-c showed similar trend, of which the *p* light diffraction efficiency (η_p) was greater than the *s* light diffraction efficiency (η_s) for sample **a1**, **a2** and **b1** whereas Fig. 5d showed the *s* light diffraction efficiency for sample **b2** was larger than *p* light diffraction efficiency during the HPDLC fabrication process. The diffraction efficiencies at different polarization states for each sample are listed in Table 1. For mixture A (DPHPA/PDDA based), the grating optical sensitivity (η_p/η_s) of **a1** and **a2** was 43.5 and 40.9 respectively. However, for mixture B (only PDDA based), the grating optical sensitivity η_p/η_s of **b1** and **b2** was 19.1 and 1/35.8 respectively. This also means the surface anchoring effect of the alignment PI layer is dominant in **b2**, which makes the majority of phase separated LCs to be aligned by the designed rubbing direction, as indicated in Fig. 1b.

In order to understand the difference of diffraction efficiency in **b2**, we adopt a coordinate system with x in the direction of the grating vector and y perpendicular to the cell surface. The diffraction efficiency for each polarization at the Bragg angle (θ_B) follows the equations[18]

$$\eta_p = \sin^2 \frac{\pi d(\varepsilon_{1x} \cos^2 \theta_B - \varepsilon_{1y} \sin^2 \theta_B)}{2n\lambda_0 \cos \theta_B} \quad (1)$$

$$\eta_s = \sin^2 \frac{\pi d \varepsilon_{1z}}{2n\lambda_0 \cos \theta_B} \quad (2)$$

where $\varepsilon_{1i}(i = x, y, z)$ is the diagonal components of the relative permittivity modulation tensor, d is the cell gap, n is the average refractivity of the grating and λ_0 is the wavelength of the probe light (633 nm, He-Ne laser). θ_B is 22° in our experiment. As the value of θ_B is small, Eqs. (1) and (2) can be simplified as

$$\eta_p = \sin^2 \frac{\pi d \varepsilon_{1x}}{2n\lambda_0} \quad (3)$$

$$\eta_s = \sin^2 \frac{\pi d \varepsilon_{1z}}{2n\lambda_0} \quad (4)$$

We can see, as the refractive index of pure polymer ($n_p = 1.525$ for mixture A, $n_p = 1.529$ for mixture B, both measured by an Abbe refractometer) is close to the ordinary refractive index of the LC ($\mathrm{n_o} = 1.522$), the change of the diffraction efficiency at *s* or *p* polarization state is mainly related with extraordinary refractive index of the LC, i.e., the orientation of the phase seperated LC molecules. From Eqs. (3) and (4) we can conclude that the reason that η_p or η_s increases with curing time is due to the extent to which the LC is aligned along the x axis (for η_p increasing case, Fig. 1a) or z axis (for η_s increasing case, Fig. 1b).

On the other hand, the amplitude of the HPDLC diffraction efficiency is related with refractive index difference between LC and polymer. The refractive index difference Δn can be deduced by Kogelnik's isotropic coupled wave theory[19]

$$\Delta n = \frac{\lambda_0 \cos \theta_B \arcsin \sqrt{\eta_s}}{\pi d} \quad (5)$$

From Eqs. (5), we can note that higher η_s can be from larger refractive index difference, which will give more effective light feedback when pumping. It also shows the more the LC molecules aligned along the z axis, the better the feedback for the lasing output. According to Eq. (5) and measured η_s, the refractive index modulation Δn can be increased from 0.0036 (in sample **a1**) to a relatively high value of 0.0236 (in sample **b2**).

3.3 Driving voltage of HPDLC

In HPDLCs, the surface anchoring effect of the polymer plays a key role to dictate the electro-optical properties.[20] If the anchoring strength between polymer and phase separated LC molecules is weak, smaller driving voltage is required to re-orient the LC molecules with applied field. In this work, there is a competitive relationship between surface anchoring of the polymer filaments or fibers in rich-LC region (indicated in Fig.1) and anchoring effect of the alignment PI layer for sample **a2** and **b2**. Fig. 5 shows the comparison of the diffraction efficiency as a function of driving electric field for sample **a1-b2**. The driving electric field E_{90} is defined here as the electric field required attaining 90% diffraction of the first order diffraction light from 100% (without applying electric field). The E_{90} of sample **a1, a2 and b1** are 5.2 $V/\mu m$, 6.0 $V/\mu m$, and 2.0 $V/\mu m$, respectively and the E_{90} of sample **b2** is 3.0 $V/\mu m$. The results indicate that the surface anchoring energies of the polymer in sample **a1** and **a2** are greater than that in sample **b1** and **b2.** We think that it is caused by different functions of the monomers, meaning, multifunctional monomer will produce more polymer filaments in rich-LC regions and more anchoring energy than lower functional monomer. Because of the monomer with lower functionality (mixture B), the surface anchoring strength of the polymer is much smaller. Therefore the alignment PI layer in sample **b2** can be dominant for the orientation of phase separated LC molecules. Such orientation of the LC will benefit to larger Δn so that the lasing output threshold can be lower when pumping because of more efficient light feedback.

3.4 Lasing output

The samples were then photo-pumped to investigate the lasing output for DFB laser application. The pumping laser wavelength was 532 nm and the pumping direction was normal to the glass substrate of the sample. The lasing output from our samples were around 630 nm. The DFB lasing wavelength λ_{las} from the device should satisfy the Bragg condition[21] $m\lambda_{las} = 2n_{eff}\Lambda$, where n_{eff} is the effective refractive index of the laser mode and m is the Bragg order, which was selected as 3 for each sample in this work. There were four lasing output beams with equal intensity from one sample and each beam was emitted at ~32° with respect to the normal of the glass plane. The emitted lasing output beams are totally TE polarized.

Fig. 7 shows the dependence of output energy on input energy for sample **a1-b2**. The threshold of the lasing output was obtained by the intersection of the linear fitting curve. The threshold is 0.71 μJ (i.e., pump energy density 0.142 mJ/cm^2 or perk power density per pump laser pulse 17.75 kW/cm^2, the same as below) for sample **a1**, 0.74 μJ (0.148 mJ/cm^2 or 18.5 kW/cm^2) for sample **a2**, and 0.68 μJ (0.136 mJ/cm^2 or 17 kW/cm^2) for sample **b1**. The conversion efficiency of pump input to the lasing output of sample **a1**, **a2** and **b1** are 2.3%, 2.5% and 1.9%, respectively. The values of both threshold and conversion efficiency of the three samples are almost same. However, the lasing output properties of sample **b2** was greatly improved, as is shown in Fig. 7d. The value of refractive index contrast is improved from 0.0036 (sample **a1**) to 0.0236. The threshold was decreased to 0.25 μJ (0.05 mJ/cm^2 or 6.25 kW/cm^2) and the conversion efficiency was increased to 4.6%. The insets in Fig. 7 show the corresponding lasing spectra of sample **a1-b2**, respectively. Lasing with narrow linewidth was observed and their full width at half maximum (FWHM) was 0.5 nm - 0.6 nm, which showed the small difference of the lasing wavelengths in sample **a1** and **b1** can be attributed to the different kinds of the mixture being used. The lasing peak change from 630.4 nm (sample **b1**) to 632.2 nm (sample **b2**) can be attributed to the difference in the average refractive index in the HPDLC grating due to different orientation of LC molecules caused by PI alignment layer.

These results show that the lasing threshold can be lowered and the conversion efficiency can be

increased by the rubbed PI layer to control the phase separated LCs aligned in the preferred direction in the sample with low functionality of the monomer mixture. The reason is that, when the phase separated LC is aligned along rubbing direction (z), the refractive index difference in grating vector direction (x) comes from polymer (for example, n_p=1.529 for mixture B) and LC extraordinary refractive index (n_e), which was measured as 0.0236 in sample B2. Whereas in sample B1, the refractive index difference in grating vector direction is 0.0036 as the phase separated LC is aligned along grating vector direction and the refractive index of LC is ordinary refractive index (n_o, and n_o<n_e) in that case. The bigger the refractive index in grating vector direction (the lasing feedback direction), the better the lasing feedback performance. Therefore the lasing threshold and conversion efficiency can be enhanced in this work.

4. Conclusions

In this paper, we studied the effects of the alignment PI layer on lasing output threshold and conversion efficiency based on HPDLC/core-layer/glass-substrate laser configuration. The effect of different monomers, the orientation of the LC molecules in different HPDLCs and the lasing output properties were investigated. The results indicate the surface anchoring energy of the polymer in HPDLC can be suppressed by using lower functional monomer and rubbing PI alignment layer on the substrate, making LC molecules align along the designed rubbing direction. In this way, we greatly lowered the lasing output threshold and increased conversion efficiency. The obtained HPDLC also has lower light loss, higher diffraction efficiency and lower driving voltage, which is boosted as more effectively, external light feedback layer for organic semiconducting lasers.

Acknowledgements

The authors would like to thank the support from the National Natural Science Foundation of China (11174274, 11204299, 61377032, and 61378075).

References

1. (a) H. H. Telle, A. G. Urena and R. J. Donovan, *Laser Chemistry: Spectroscopy, Dynamics and Applications*, John Wiley & Sons, West Sussex, 2007; (b) W. M. Steen and J. Mazumder, *Lasers Material Processing (4th Edition)*, Springer, London, 2010; (c) N. Tessler, *Adv. Mater.*, 1999, **11**, 363-370; (d) J. Clark and G. Lanzani, *Nat. Photonics*, 2010, **4**, 438-446.

2. Y. Yang, G. A. Turnbull and I. D. W. Samuel, *Appl. Phys. Lett.*, 2008, **92**, 163306.

3. (a) T. Riedl, T. Rabe, H.-H. Johannes, W. Kowalsky, J. Wang, T. Weimann, P. Hinze, B. Nehls, T. Farrell and U. Scherf, *Appl. Phys. Lett.*, 2006, **88**, 241116; (b) C. Karnutsch, M. Stroisch, M. Punke, U. Lemmer, J. Wang and T. Weimann, *IEEE Photonics Technol. Lett.*, 2007, **19**, 741-743.

4. (a) M. D. McGehee and A. J. Heeger, *Adv. Mater.*, 2000, **12**, 1655-1668; (b) D. T. McQuade, A. E. Pullen and T. M. Swager, *Chem. Rev.*, 2000, **100**, 2537-2574.

5. S. Klinkhammer, X. Liu, K. Huska, Y. S. Vanderheiden, S. Valouch, C. Vannahme, S. Brase, T. Mappes and U. Lemmer, *Opt. Express*, 2012, **20**, 6357-6364.

6. R. Xia, G. Heliotis, P. Stavrinou and D. Bradley, *Appl. Phys. Lett.*, 2005, **87**, 031104.

7. M. G. Ramirez, P. G. Boj, V. Navarro-Fuster, I. Vragovic, J. M. Villalvilla, I. Alonso, V. Trabadelo, S. Merino and M. A. Diaz-Garcia, *Opt. Express*, 2011, **19**, 22443-22454.

8. B. Wenger, N. Tetreault, M. E. Welland and R. H. Friend, *Appl. Phys. Lett.*, 2010, **97**, 193303.

9. M. Gaal, C. Gadermaier, H. Plank, E. Moderegger, A. Pogantsch, G. Leising and E. J. W. List, *Adv. Mater.*, 2003, **15**, 1165-1167.

10. T. Zhai, X. Zhang, Z. Pang and F. Dou, *Adv. Mater.*, 2011, **23**, 1860-1864.

11. I. D. W. Samuel and G. A. Turnbull, *Chem. Rev.*, 2007, **107**, 1272-1295.

12. G. Heliotis, R. Xia, G. A. Turnbull, P. Andrew, W. L. Barnes, I. D. Samuel and D. D. Bradley, *Adv. Funct. Mater.*, 2004, **14**, 91-97.

13. (a) Z. Diao, L. Xuan, L. Liu, M. Xia, L. Hu, Y. Liu and J. Ma, *J. Mater. Chem. C*, 2014, **2**, 6177-6182; (b) W. Huang, Z. Diao, Y. Liu, Z. Peng, C. Yang, J. Ma and L. Xuan, *Org. Electron.*, 2012, **13**, 2307-2311.

14. (a) T. J. Bunning, L. V. Natarajan, V. P. Tondiglia and R. L. Sutherland, *Annu. Rev. Mater. Sci.*,

2000, **30**, 83-115; (b) R. L. Sutherland, V. P. Tondiglia, L. V. Natarajan, T. J. Bunning and W. W. Adams, *Appl. Phys. Lett.*, 1994, **64**, 1074-1076; (c) C. Y. Li, M. J. Birnkrant, L. V. Natarajan, V. P. Tondiglia, P. F. Lloyd, R. L. Sutherland and T. J. Bunning, *Soft Matter*, 2005, **1**, 238-242; (d) Y. J. Liu, Y.-C. Su, Y.-J. Hsu and V. K. Hsiao, *J. Mater. Chem.*, 2012, **22**, 14191-14195; (e) Y. J. Liu, H. T. Dai and X. W. Sun, *J. Mater. Chem.*, 2011, **21**, 2982-2986; (f) L. De Sio, L. Ricciardi, S. Serak, M. La Deda, N. Tabiryan and C. Umeton, *J. Mater. Chem.*, 2012, **22**, 6669-6673; (g) R. Caputo, L. De Sio, A. Veltri, C. Umeton and A. V. Sukhov, *Opt. Lett.*, 2004, **29**, 1261-1263; (h) V. K. S. Hsiao, K.-T. Yong, A. N. Cartwright, M. T. Swihart, P. N. Prasad, P. F. Lloyd and T. J. Bunning, *J. Mater. Chem.*, 2009, **19**, 3998-4003.

15. (a) J. Ma, W. Huang, L. Xuan and H. Yokoyama, in *Optical Properties of Functional Polymers and Nano Engineering Applications*, eds. V. Jain and A. Kokil, CRC, 2014; (b) L. Liu, W. Huang, Z. Diao, Z. Peng, Q. q. Mu, Y. Liu, C. Yang, L. Hu and L. Xuan, *Liq. Cryst.*, 2014, **41**, 145-152; (c) Z. Diao, W. Huang, Z. Peng, Q. Mu, Y. Liu, J. Ma and L. Xuan, *Liq. Cryst.*, 2014, **41**, 239-246; (d) Z. Diao, S. Deng, W. Huang, L. Xuan, L. Hu, Y. Liu and J. Ma, *J. Mater. Chem.*, 2012, **22**, 23331-23334; (e) W. Huang, Z. Diao, L. Yao, Z. Cao, Y. Liu, J. Ma and L. Xuan, *Applied Physics Express*, 2013, **6**, 022702; (f) W. Huang, Y. Liu, Z. Diao, C. Yang, L. Yao, J. Ma and L. Xuan, *Appl. Opt.*, 2012, **51**, 4013-4020.

16. V. K. S. Hisao, C. Lu, G. S. He, M. Pan, A. N. Cartwright, P. N. Prasad, R. Jakubiak, R. A. Vaia and T. J. Bunning, *Opt. Express*, 2005, **13**, 3787-3794.

17. (a) R. T. Pogue, L. V. Natarajan, S. A. Siwecki, V. P. Tondiglia, R. L. Sutherland and T. J. Bunning, *Polymer*, 2000, **41**, 733-741; (b) M. D. Sarkar, J. Qi and G. P. Crawford, *Polymer*, 2002, **43**, 7335-7344.

18. J. J. Butler, M. S. Malcuit and M. A. Rodriguez, *J. Opt. Soc. Am. B: Opt. Phys.*, 2002, **19**, 183-189.

19. H. Kogelnik, *Bell Syst. Tech. J.*, 1969, **69**, 2909-2946.

20. (a) R. Jakubiak, V. P. Tondiglia, L. V. Natarajan, R. L. Sutherland, P. Lloyd, T. J. Bunning and R.

A. Vaia, *Adv. Mater.*, 2005, **17**, 2807-2811; (b) R. Jakubiak, T. J. Bunning, R. A. Vaia, L. V. Natarajan and V. P. Tondiglia, *Adv. Mater.*, 2003, **15**, 241-244; (c) K. K. Vardanyan, J. Qi, J. N. Eakin, M. D. Sarkar and G. P. Crawford, *Appl. Phys. Lett.*, 2002, **81**, 4736-4738; (d) H. Ren and S. T. Wu, *J. Appl. Phys.*, 2002, **92**, 797-800; (e) J. Ma, L. Shi and D.-K. Yang, *Applied Physics Express*, 2010, **3**, 021702. (f) S. E. Hicks, S. P. Hurley, Y. C. Yang and D.-K. Yang, *Soft Matter*, 2013, **9**, 3834-3839; (g) M. E. McConney, T. J. White, V. P. Tondiglia, L. V. Natarajan, D.-K. Yang and T. J. Bunning, *Soft Matter*, 2012, **8**, 318-323. (h) D.-K. Yang and S.-T. Wu, *Fundamentals of Liquid Crystal Devices*, John Wiley & Sons Inc, New York, 2006.

21. H. Kogelnik and C. V. Shank, *J. Appl. Phys.*, 1972, **43**, 2327-2335.

Table and Figures

Table 1 Illustration and properties of samples.

Fig. 1 Device structures of (a) without PI alignment layer and (b) with PI alignment layer.

Fig. 2 Chemical structures of (a) DPHPA and (b) PDDA.

Fig. 3 Optical setup for fabrication and characterization of HPDLC grating.

Fig. 4 Evolution of the light loss for *p* polarization (square) and *s* polarization (sphere) with curing time for (a) **a1**, (b) **a2**, (c) **b1** and (d) **b2**, respectively.

Fig. 5 Real time diffraction efficiency for *p* polarization (square) and *s* polarization (sphere) for (a) **a1** (b) **a2**, (c) **b1** and (d) **b2**, respectively.

Fig. 6 Diffraction efficiency as a function of applied electric field for (a) **a1**, (b) **a2**, (c) **b1** and (d) **b2**, respectively.

Fig. 7 Lasing output intensity as a function of pump intensity for the DFB laser: (a) **a1**, (b) **a2**, (c) **b1** and (d) **b2**. The insets show the corresponding lasing spectra, respectively.

Table 1 Illustration and properties of samples.

Sample #	Mixture	Top glass substrate	η_p (%)	η_s (%)	η_p / η_s
a1	A	bare glass	56.5	1.3	43.5
a2	A	coated with PI and rubbed	57.2	1.4	40.9
b1	B	bare glass	55.5	2.9	19.1
b2	B	coated with PI and rubbed	1.6	57.3	1/35.8

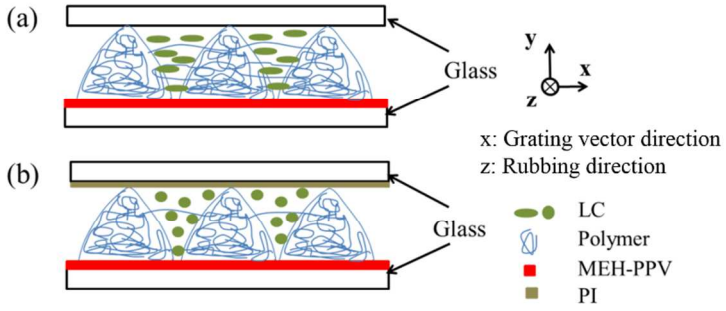

Fig. 1 Device structures of (a) without PI alignment layer and (b) with PI alignment layer.

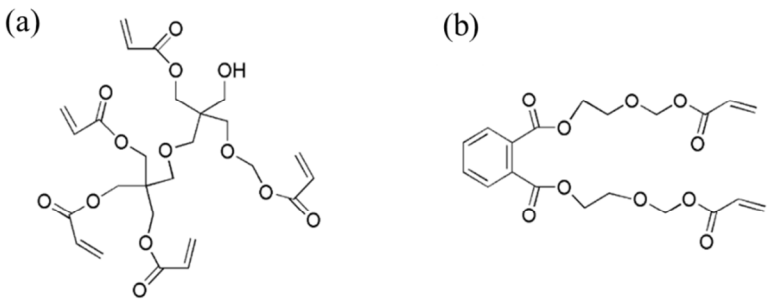

Fig. 2 Chemical structures of (a) DPHPA and (b) PDDA.

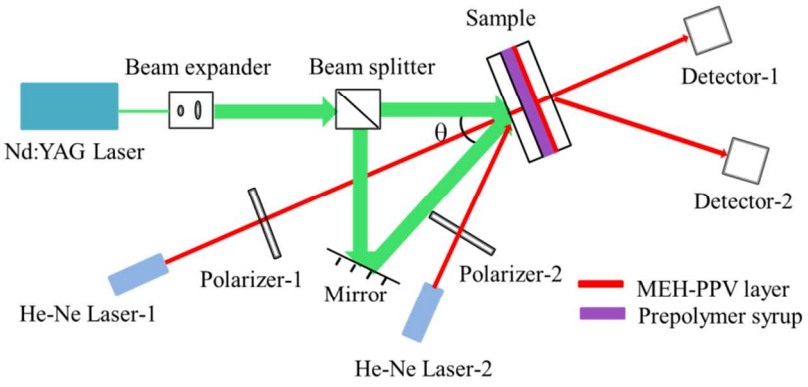

Fig. 3 Optical setup for fabrication and characterization of HPDLC grating.

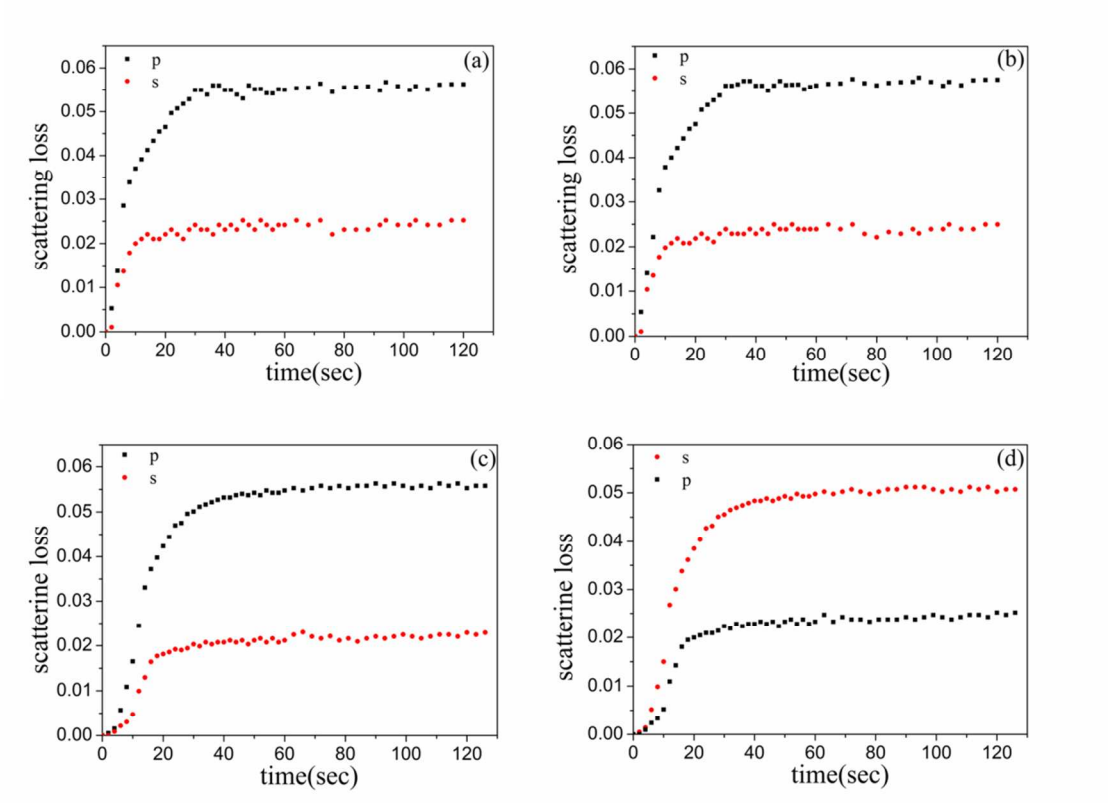

Fig. 4 Evolution of the light loss for *p* polarization (square) and *s* polarization (sphere) with curing time for (a) **a1**, (b) **a2**, (c) **b1** and (d) **b2**, respectively.

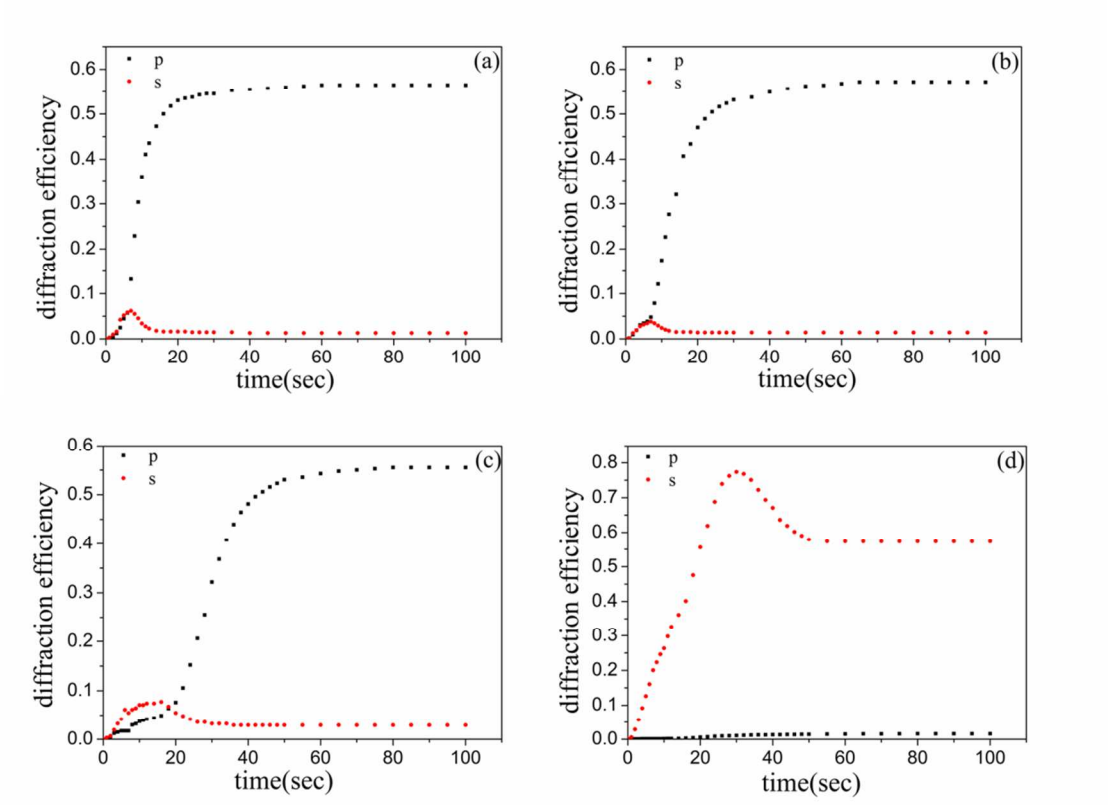

Fig. 5 Real time diffraction efficiency for *p* polarization (square) and *s* polarization (sphere) for (a) **a1** (b) **a2**, (c) **b1** and (d) **b2**, respectively.

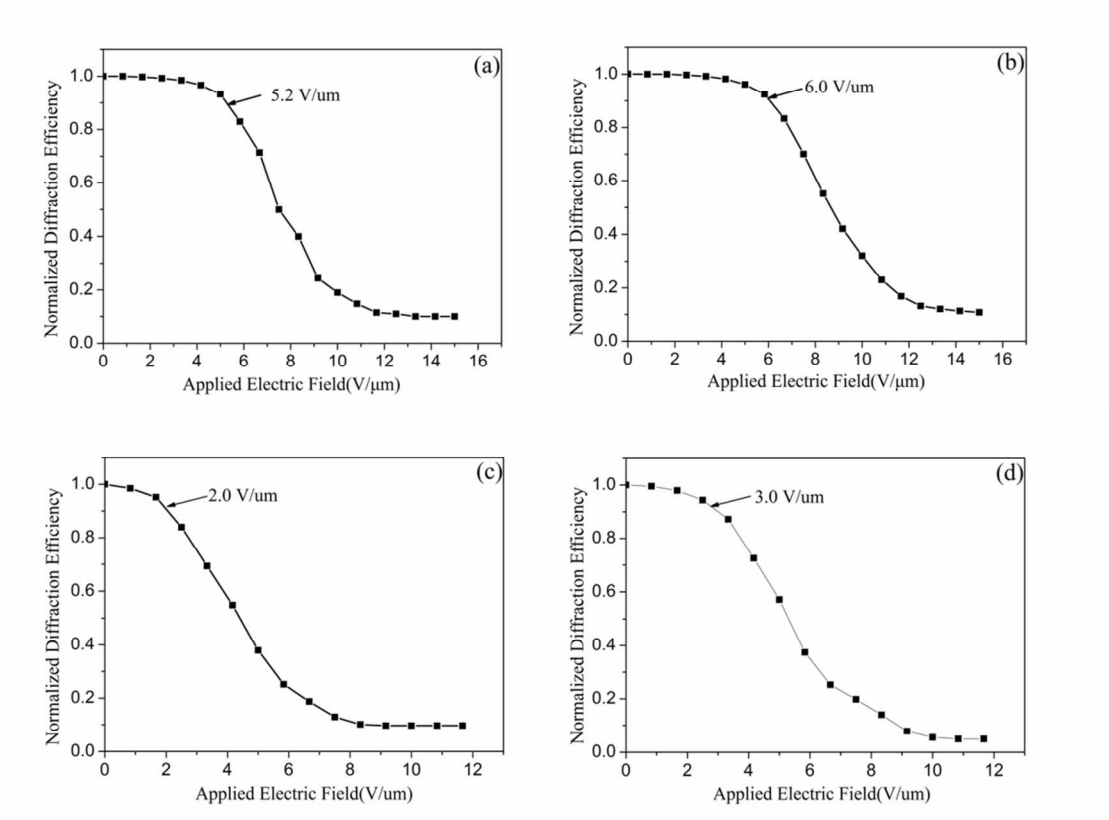

Fig. 6 Diffraction efficiency as a function of applied electric field for (a) **a1**, (b) **a2**, (c) **b1** and (d) **b2**, respectively.

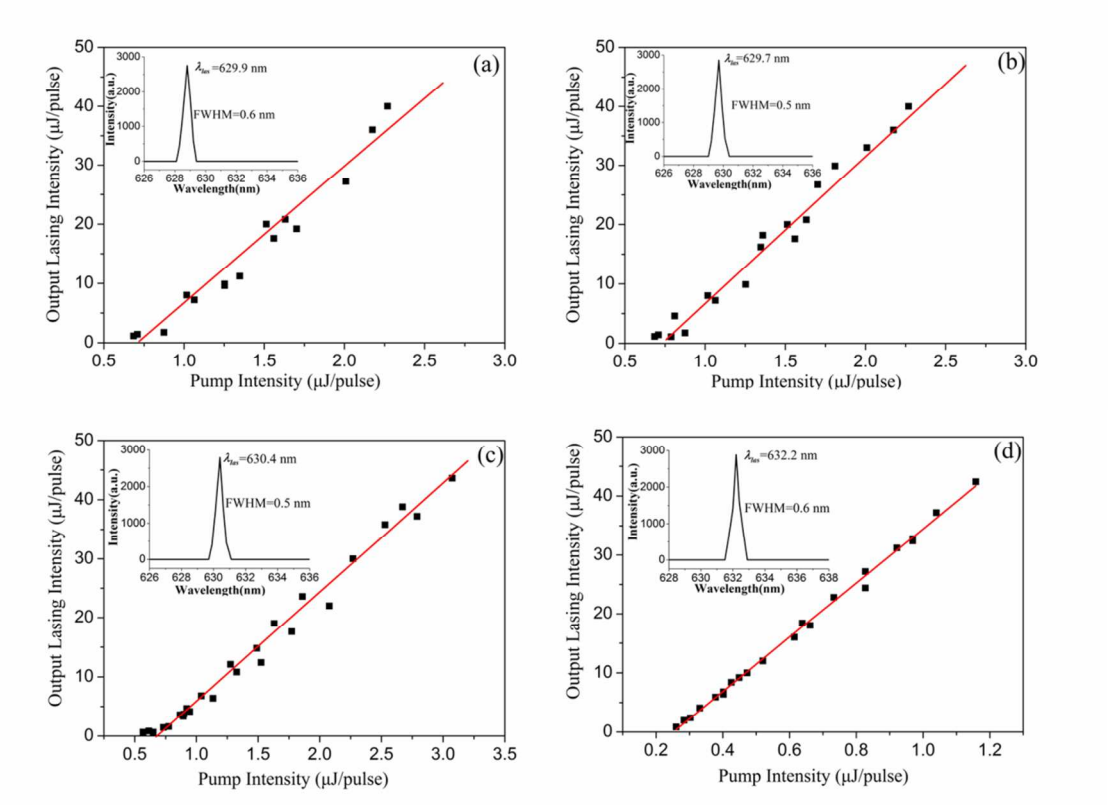

Fig. 7 Lasing output intensity as a function of pump intensity for the DFB laser: (a) **a1**, (b) **a2**, (c) **b1** and (d) **b2**. The insets show the corresponding lasing spectra, respectively.

Graphical Abstract

A low threshold, high energy conversion organic distributed feedback (DFB) laser based on a holographic polymer dispersed liquid crystal (HPDLC) grating, as the external light feedback layer, with preferred LC molecular orientation was reported to provide better light feedback.